Design of Hydrophobic Polyoxometalate Hybrid Assemblies Beyond Surfactant Encapsulation

Yu-Fei Song,[a] Nicola McMillan,[a] De-Liang Long,[a] Johannes Thiel,[a] Yulong Ding,[b] Haisheng Chen,[b] Nikolaj Gadegaard,[c] and Leroy Cronin*[a]

Abstract: Grafting of C-6, C-16 and C-18 alkyl chains onto the hydrophilic Mn-Anderson clusters (compounds **2–4**) has been achieved. Exchange of the tetrabutyl ammonium (TBA) with dimethyldioctadecyl ammonium (DMDOA) results in the formation of new polyoxometalate (POM) assemblies (compounds **5–6**), in which the POM cores are covalently functionalized by hydrophilic alkyl-chains and enclosed by surfactant of DMDOABr. As a result, we have been able to design and synthesize POM-containing hydrophobic materials beyond surfactant encapsulation. In solid state, scanning electron and transmission electron microscopy (SEM and TEM) studies of the TBA salts of compounds **3** and **4** show highly ordered, uniform, reproducible assemblies with unique segmented rodlike morphology. SEM and TEM studies of the DMDOA salts of compounds **5** and **6** show that they form spherical and sea urchin 3D objects in different solvent systems. In solution, the physical properties of compound **5** and **6** (combination of surfactant-encapsulated cluster (SEC) and surface-grafted cluster (SGC)) show a liquid-to-gel phase transition in pure chloroform below 0°C, which are much lower than other reported SECs. By utilizing light scattering measurements, the nanoparticle size for compounds **5** and **6** were measured at 5°C and 30°C, respectively. Other physical properties including differential scanning calorimetry have been reported.

Keywords: hydrophobic materials · organic–inorganic hybrid composites · phase transitions · polyoxometalates · surfactant encapsulation

Introduction

Polyoxometalates (POMs) are metal-oxide clusters[1] of V, Mo, W etc. and represent a class of inorganic materials with an almost unmatched range of structure types and physical properties with applications in areas as diverse as biology[2] and catalysis.[3] Polyoxometalate clusters cover an enormous size range and comprise conserved/transferable building blocks; it is this feature that means they hold considerable promise for the controlled assembly of large nanostructures and framework materials.[4] The synthesis of organic–inorganic hybrid POMs has attracted widespread attention in the domain of materials science since the nanoscale clusters, which are highly anionic, are perfect scaffolds for the development of hybrid assemblies, though direct covalent modification of POMs is rare and only a few POM clusters including $[Mo_6O_{19}]^{2-}$,[5] α_1/α_2-$[P_2W_{17}O_{61}]^{10-}$,[6–7] some organophosphoryl[8] and organosilyl[9] derivatives of lacunary POM clusters have been covalently functionalized to date.[10] As these hybrid materials will combine not only the advantages of organic components and inorganic clusters, but also the close interaction and synergistic effect between them, it is of great interest to develop such organic–inorganic hybrids through covalent functionalization.

Recently, cationic surfactants have been applied to assembly with POM clusters [11] and the resulting surfactant-encapsulated clusters (SECs) are compatible with organic functional groups, which have been successfully assembled into polymeric[12] and liquid crystalline materials.[13] These materials show it is possible to retain the basic physical and chemical properties of the POM clusters, however, it should be emphasized that mainly electrostatic interactions exist

[a] Dr. Y.-F. Song, N. McMillan, Dr. D.-L. Long, J. Thiel, Prof. Dr. L. Cronin
WestCHEM, Department of Chemistry
University of Glasgow, G12 8QQ (UK)
Fax: (+44)141-330-4888
E-mail: L.Cronin@chem.gla.ac.uk

[b] Dr. Y. Ding, Dr. H. Chen
Institute of Particle Science, Department of Engineering
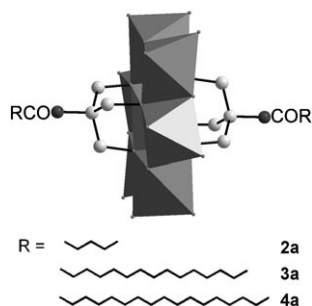University of Leeds, LS2 9JT, Leeds (UK)

[c] Dr. N. Gadegaard
Department of Electronics and Electrical Engineering
University of Glasgow, G12 8QQ (UK)

Supporting information for this article is available on the WWW under http://www.chemeurj.org/ or from the author.

between the organic functional group and POM clusters.[14–18]

In recent years, considerable attention has been paid to the amphiphilic molecules incorporated with functional units, which can result in the formation of assemblies with novel physical properties.[19] Previous studies have shown that a variety of units such as oligo(*p*-phenylene vinylene),[20] thiophene,[21] fullerene[22] and metal ions can be utilized to fabricate functional amphiphiles.[23] Nevertheless, examples with polyoxometalates have rarely been reported, despite their versatile nature. In the few related papers of POM-containing hydrophobic materials reported so far,[11] the POM hybrids have been obtained through surfactant encapsulation and mainly electrostatic interactions exist between POM and surfactant molecules. In parallel to these studies, we have been interested in developing POM hybrid assemblies by covalently anchoring organic groups to POM clusters in order to engineer new physical properties and in exploiting the development of synergistic effects between the different functional groups.

In this contribution, we focus on developing microstructures of inorganic oxides mediated by hydrophobic and hydrophilic interactions. We have been able to synthesize organic–inorganic hybrids by grafting Tris (Tris = tris(hydroxymethyl)amino methane, $[(HOCH_2)_3CNH_2]$), onto the Mn-Anderson cluster via the alkoxo groups. The "free" reactive group -NH_2 on the other side of the Tris presents a route[24–25] to develop a new type of POM-containing materials. As a result, we have successfully grafted long (C-16 and C-18, see Scheme 1) alkyl-chains through covalent amide

$\{(OCH_2)_3NH\text{-}CO\text{-}(CH_2)_{14}\text{-}CH_3\}_2]^{3-}$ (C-16) and **4a** $[MnMo_6O_{18}\{(OCH_2)_3NH\text{-}CO\text{-}(CH_2)_{16}\text{-}CH_3\}_2]^{3-}$ (C-18), have been synthesized as TBA salts by reaction of $[TBA]_3$-$[MnMo_6O_{18}\{(OCH_2)_3NH_2\}_2]$ (compound **1**) with the corresponding acetyl chloride agents. Ion exchange of the **3** and **4** with the surfactant dimethyldioctadecylammonium bromide (DMDOABr) yields compounds $[3a(DMDOA)_3]$ (**5**) and $[4a(DMDOA)_3]$ (**6**) respectively. It should be noted that the alkyl chains have been tethered to the Mn-Anderson cluster through the tris (tris(hydroxymethyl)-aminomethane, $(HOCH_2)_3NH_2)$ coupling unit and as a result, compounds **3**–**4** represent the first examples of POM-based hybrids with a cluster core connected covalently to long alkyl-chains giving POM-hybrid assemblies with both hydrophilic (Mn-Anderson cluster) and hydrophobic (long alkyl-chains) properties.

Compounds **2**–**6** have been fully characterized by IR, NMR, and elemental analysis and by cryospray mass spectroscopy. Structural analysis of compounds **3** and **4** gave unit cell parameters that were slightly different within $\pm 2\%$ $((49.590–50.20) \times (28.51–28.61) \times (25.59–25.68);$ $90 \times (99.8–101.0) \times 90^\circ;$ $V = 35649–36202$ Å^3; $z = 14$) in chain length, but otherwise the structures were almost identical. The main structure and TBA cation can be located clearly. However, as expected, there is an exceptional amount of disorder associated with the many possible conformations of the long alkyl-chains and only the first 5–6 carbon atoms can be located (see Figure S1 in the Supporting Information). Compound **2** has been characterized by single-crystal X-ray structural measurement. The structure[26] of compound **2** is well defined (see Figure 1), and comprises the $[MnMo_6O_{18}$-$\{(OCH_2)_3NH\}_2]^{3-}$ cluster core with C-6 chains appended to both sides of the cluster units. It is interesting to note that each C-6 chain has a different conformation with one of the C-6 chains adopting a bent conformation whereas the other one adopts a more conventional chain conformation. Impor-
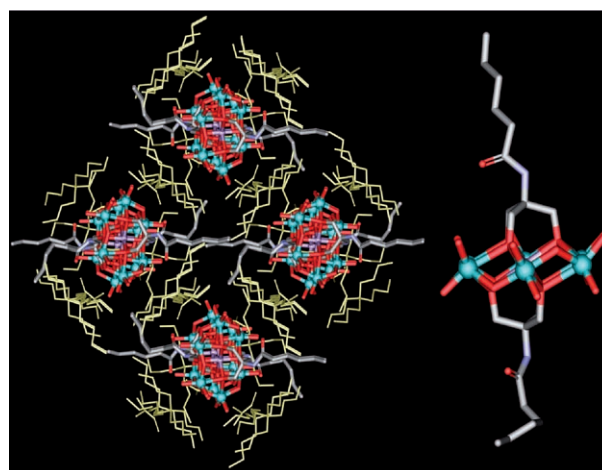
Scheme 1. Formation of Compounds **2a**–**4a** (**a** denotes anion).

bonds to the Mn-Anderson cluster with the aim to develop robust POM-containing hybrid assemblies of surface-grafted clusters (SGCs). In addition, cation exchange of POMs clusters from tetrabutyl ammonium (TBA; compounds **3**, **4**) to dimethyldioctadecyl ammonium (DMDOA; compounds **5**, **6**) leads to hydrophobic POM hybrids with the combination of SECs and SGCs.

Results and Discussion

Three new Mn-Anderson anions; **2a** $[MnMo_6O_{18}$-$\{(OCH_2)_3NH\text{-}CO\text{-}(CH_2)_4CH_3\}_2]^{3-}$ (C-6), **3a** $[MnMo_6O_{18}$-

Figure 1. Structure of compound **2** (left), $[MnMo_6O_{18}\{(OCH_2)_3NH\text{-}CO\text{-}(CH_2)_4\text{-}CH_3\}_2](TBA)_3$; the TBA cations are shown in yellow, the C-6 chain in grey and the cluster core in green, purple (Mo, Mn) and red (O). The structure of **2a** (right) shows the two appended C-6 chains in detail.

tantly, the X-ray crystal structure study of compound **2** demonstrates that the alkyl chain is attached to the cluster via the tris coupling unit. The appearance of the six carbon atoms in the structural analysis of compounds **3**–**4**, combined with the MS spectra results of compounds **3**–**4** (see Figures S2 and S3 in the Supporting Information) and the well-defined structure of compound **2**, provide definitive proof for the formation of the amide bond and the covalent attachment of the long alkyl-chains to Mn-Anderson clusters in compounds **3**–**4**.

To investigate the structures of compounds **3** and **4**, deposition of both compounds on silicon surfaces generates long, uniformly segmented, micro-scale 1D rods. The long needle-like shape is observed in the full view for both of them (Figure 2A). Close examination of the "needle" patterns shows
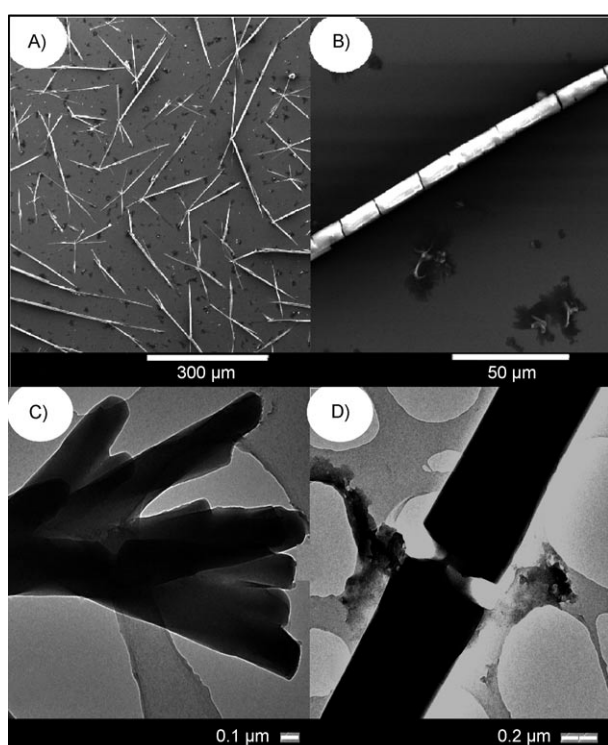

Figure 2. SEM images of compound **3**; A) prepared from CHCl$_3$ solution and B) from CHCl$_3$/MeCN = 4:1. TEM images of compound **3**; C) layered architecture and D) enlargement of one of the segmented "rods" from the layered structure.

that they are all composed by highly ordered, segmented rods with length in the range of 100–500 μm and width of 5–10 μm (Figure 2B). The scanning electron microscopy (SEM) results demonstrate that both of the assemblies have an unique 1D segmented rod morphology, which is presumably directed by crystallization of compound **3** and **4** on the surface. The arrangement of these segmented micro-scale rods are well organized on the silicon surface and the size of each fragment is around 10–25 μm long and 5–10 μm wide on average. The 1D micro-scale rods were further character-

ized by transmission electron microscopy (TEM) and the result is consistent with the observations from the SEM.

It is very interesting that the anisotropic clusters of **3** and **4** also form anisotropic features on the surface, therefore, studies were also conducted on compounds **5** and **6**, which are DMDOA salts of **3a** and **4a**, respectively. The incorporation of surfactant cations, containing C-18 chains, into the overall salts of **3a** and **4a** offers many advantages, including making the POM extremely soluble in CHCl$_3$ and allows the generation of core–shell hydrophilic–hydrophobic surfactant-encapsulated clusters (SEC) as well as surface-grafted clusters (SGC). The resultant assemblies in **5** and **6** include three DMDOA cations and each of them contains two hydrophobic C-18 chains on the quaternary nitrogen. Additionally, there are two hydrophobic C-16 or C-18 chains covalently tethered to the Mn-Anderson cluster cores in **5** and **6** respectively.

If prepared from pure chloroform, compound **5** shows 3D spherical morphology, 1 μm to 20 μm in size. Increasing the polarity of the solvent by addition of acetonitrile to the chloroform solution can alter the morphology to produce more ordered, sea urchin-like aggregates with the long needles extending out from the core in different directions (see Figure 3). The surface behaviors of compound **5** and **6** show significant differences from the "honeycomb" morphology of other SECs[11] reported. In contrast to the SEM images of
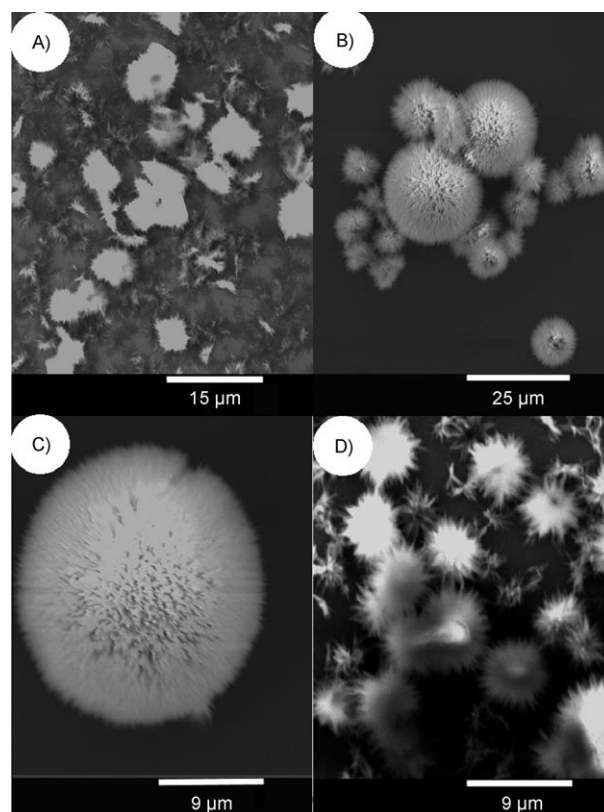

Figure 3. SEM image of compound **5** A) prepared from CHCl$_3$ solution and B) prepared from CHCl$_3$/MeCN = 4:1. C) A magnified image of compound **5** in B). D) Compound **6** prepared from CHCl$_3$/MeCN = 4:1.

compounds **3** and **4**, the SEM images of compounds **5** and **6** show that the growth direction for both of them is not only within the layers of anion and cation, but also in the direction perpendicular to the layers with anisotropic features. This is because the DMDOA cations encapsulate Mn-Anderson cluster and the long alkyl-chains from DMDOA$^+$ spread over the surface of the Mn-Anderson cluster through electrostatic interactions. Typical TEM images are shown in Figure 4 obtained from solvent-cast films of compound **5/6** with the off-set multilayer architectures.
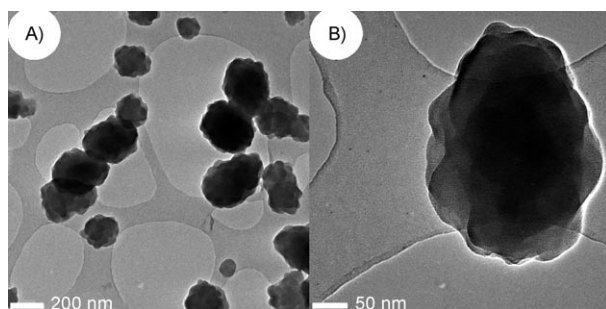

Figure 4. TEM images of compound **5**; A) full view of the uniform formation of the composite on the surface and B) a magnified image of the species appeared on the surface showing the stagger-layer morphology.

Comparison of the thermal properties of the TBA and DMDOA salts of **3a** and **4a** (i.e. compounds **3**,**4** vs. **5**,**6**) provides some interesting parallels. Firstly, both **3** and **4** have similar properties as do **5** and **6**, but the differences between each class of compound (TBA vs. DMDOA salt) is dramatic (see Figure 5). Although compounds **3–6** appear to decompose around 250°C (Figure S9 in the Supporting Information), changing the TBA to DMDOA gives a very sharp "melting" like transition at 62°C. Further coupled heating and cooling studies show that there is also an associated "crystallization" process (Figure S10 in the Supporting Information) upon cooling for compounds **5–6** at 45°C. This can be compared to (DMDOABr) which features a sharp "melting" peak at 90°C and "crystallization" process at 75°C so it is interesting that the melting process for compounds **5–6** is depressed by around 30°C compared to pure DMDOABr. The "reversible" phase transition is caused by the transformation of one dimensional lamellae of
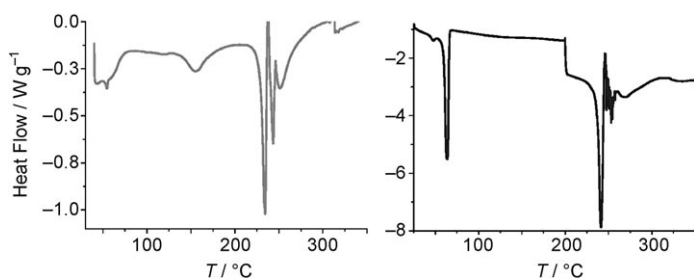
DMDOA$^+$, in which the hydrocarbon chains are fully extended and somewhat tilted, to two-dimensional structures with hydrocarbon chains distorted by undulations.[27] The difference of the phase transition temperatures between DMDOABr and compound **5–6** is a result of the interactions between DMDOA$^+$ and anionic Mn-Anderson clusters in compound **5–6**.

Because the phase transitions of the alkyl chains from gel to liquid-crystalline state for the conventional vesicles prepared by synthetic surfactants or lipids take place during the heating process,[28–29] we also studied the physical properties of **5** and **6** in solution and as a function of solvent polarity. We found that upon heating, both compounds undergo phase transitions (Tc), which are dependent upon solvent polarity. The alkyl chains are quite flexible in pure chloroform with very good solubility and the corresponding Tc values of compound **5** and **6** are relatively low at −4 to −2°C and −8 to −10°C, respectively. Comparison of this data with other SECs and POM-containing SECs shows that the Tc reported here is decreased significantly in pure CHCl$_3$. Addition of acetonitrile can increase the polarity of the solvent and the hydrophobic interaction between alkyl chains. As a result, the Tc value is increased to 6–8°C and 13–15°C for compound **5** and **6**, respectively, if the volume ratio of chloroform to acetonitrile is 6:1, indicating that the DMDOA$^+$ cation chains in the assemblies undergo an essential phase transition from a gel to liquid-crystalline state. Light scattering studies on compounds **5** and **6** below the Tc (at 5°C) show the presence of large colloidal aggregates of 142 and 42 nm in size respectively for 2.8 mmol L^{-1} solutions. Furthermore, at 30°C, light scattering measurements (see Figure 6) showed the presence of particles with a diameter of between 4–5 nm for compounds **5–6**. This diameter corresponds to the end-to-end distance between two stretched C-16/C-18 chain grafted to the Mn-Anderson which is around 5–6 nm.

Figure 5. Differential scanning calorimetry thermograms of compound **3** (left) and compound **5** (right). The scan rate is 5°C min^{-1}.
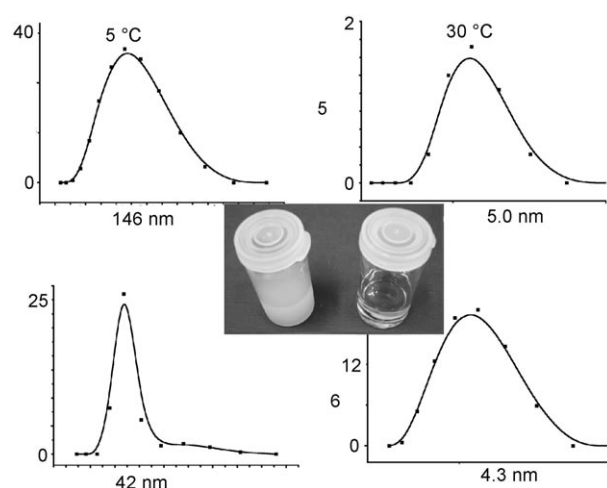

Figure 6. Light scattering measurements of **5** (top) and **6** (bottom) at 5°C (left) and 30°C (right). The modal values are given in nm and a photograph of the solution of compound **5** at 5°C (left) and 30°C (right) is shown.

It should be emphasized that several interesting features including dramatic differences from other SECs have been observed in our studies: 1) By covalently grafting long alkyl-chains onto POMs, we have been able to construct POM hybrid assemblies with hydrophilic–hydrophobic properties. The design is different from those reported in the literature. 2) The T_c values of −4 and −8 °C for compound **5** and **6** in CHCl$_3$ are much lower than those of conventional vesicles prepared by synthetic surfactants or lipids. This reflects the excellent solubility of both **5–6** in CHCl$_3$. 3) SEM images show that highly ordered, uniform, rodlike morphology for compounds **3–4**, whereas well sea urchin-like morphology for compound **5–6** from the mixture of CHCl$_3$/MeCN. These unusual surface behaviors, which are very different from the "honeycomb" or "onionlike" morphologies of DMDOABr or other SECs,[11] are caused by the existence of SGC for compound **3–4** and the co-existence of SGC-SEC for compound **5–6** considering that Mn-Anderson itself appears to be amorphous powder on the surface. 4) All of these materials (compounds **3–6**) are thermally stable to 250 °C and basic physical and chemical properties of the Mn-Anderson cluster are retained.

Conclusion

In summary, by covalently grafting long alkyl-chains onto Mn-Anderson clusters, POM-containing hydrophobic assemblies have been obtained. Controlled morphologies have been observed and some interesting physical properties including phase transition and nanoparticle measurement have been conducted. The hydrophobic POM hybrids of compounds **5–6** reported herein represent the first examples of hydrophilic–hydrophobic surface-grafted clusters as well as surfactant-encapsulated clusters with nanometer scale structures, in which POM cores are covalently functionalized by hydrophilic alkyl-chains and enclosed by surfactant DMDOA$^+$.

Experimental Section

General: All reagents and chemicals including deuterated solvents were purchased from Aldrich-Sigma Company and used without further purification. NMR spectra were recorded at Bruker DPX 400 spectrometer at room temperature (University of Glasgow). Elemental Analyses were completed by using an Elemental Analyser MOD 1106, University of Glasgow. IR spectroscopy was carried out by means of a JASCO FTIR 410 spectrometer and wave numbers ($\tilde{\nu}$) is in cm^{-1}; intensities denoted as vs = very strong, s = strong, m = medium, w = weak. X-ray crystallography diffraction data were collected by means of a Bruker Apex II CCD Difractometer (100 K). SHELXS-97 was used for structure solution and SHELXL-97 was used for refinement. The SEM (scanning electron microscopy) images were obtained by using a field emission scanning electron microscope (JROL, JSM-6400) operated at an acceleration voltage of 10 kV. The silicon substrates and samples for SEM measurements were prepared as follows: The silicon substrates were cleaned by sonication in ethanol for 20 minutes and dried under a stream of nitrogen. The solutions of compounds **3–6** were dissolved in MeCN, CHCl$_3$ or mixture of MeCN/CHCl$_3$ to 1 mg mL^{-1} according to different experimental condi-

tions and 10 μL of each of the solutions was deposited onto the substrate and dried. The TEM (transmission electron microscopy) measurements were carried out by using TEC NAI T20 with GIF 2000: Gatan Imaging Filter. The samples for TEM measurement were prepared as follows: The solutions of compound **3–6** were dissolved in a mixture of MeCN/CHCl$_3$ (1:4) to 1 mg mL^{-1} and 5 μL of the solutions were deposited onto the Cu/C substrates and dried. The size of polyoxometalate nanoscale hybrid assemblies (compound **5–6**) was characterized by dynamic light scattering (DLS) by using a Malvern Nano Sizer ZS instrument. The device is equipped with noninvasive back-scatter (NIBS) capability and detects the scattering information at 173°. In a typical measurement, a sample was put in a glass cuvette and cooled down in a laboratory freezer for an hour to below −250 K. The sample was then taken out of the freezer and allowed to warm up in the chamber of the Nano Sizer to 278 K and maintained at the temperature for 30 min before the size measurement was made. The sample was then heated up to and maintained at 303 K at which the size measurement was taken again.

[(n-C$_4$H$_9$)$_4$N]$_3$[MnMo$_6$O$_{18}${(OCH$_2$)$_3$CNH$_2$}$_2$] (compound **1**) was synthesized as described in literature[24] and fully characterized.

Synthesis of [(nC$_4$H$_9$)$_4$N]$_3$[MnMo$_6$O$_{18}${(OCH$_2$)$_3$CNH-CO-(CH$_2$)$_4$CH$_3$}$_2$]·2DMF (compound 2): Compound **1** (0.50 g, 0.27 mmol) and Et$_3$N (150 μL; 0.11 g; 1.08 mmol) were dissolved in 50 mL of acetonitrile. Hexanoyl chloride (0.071 g, 0.54 mmol) was added slowly and the reaction mixture was kept refluxing for 6 h. A white precipitate was filtered off and the filtrate was evaporated. The orange product was dissolved in a minimum amount of DMF (8 mL). Orange, needle crystals suitable for X-ray single crystal diffraction measurement were crystallized out from DMF solution after two weeks. Yield: 110 mg, (0.049 mmol, 18 %). ESI-MS (negative mode, MeCN): ([M-2DMF-H$_2$O-TAB]$^-$) 1837 g mol^{-1}; elemental analysis calcd (%) for C$_{68}$H$_{144}$MnMo$_6$N$_5$O$_{26}$·2DMF·H$_2$O (2242.67 g mol^{-1}): C 39.63, H 7.19, N 4.37; found C 39. 85, H 7.10. N 4.52.

Synthesis of [(nC$_4$H$_9$)$_4$N]$_3$[MnMo$_6$O$_{18}${(OCH$_2$)$_3$CNH-CO-(CH$_2$)$_{14}$CH$_3$}$_2$]·7H$_2$O·2DMF (compound 3): Compound **1** (0.50 g; 0.27 mmol) and Et$_3$N (150 μL; 0.11 g; 1.08 mmol) were dissolved in 30 mL of acetonitrile. Palmitoyl chloride (0.15 g; 0.53 mmol) was added slowly and the solution was kept refluxing for 10 h. A white precipitate was filtered off and the solvent was evaporated. The orange residue was dissolved in a minimum amount of DMF (10 mL). Orange crystals with long, needle shape were obtained by ether diffusion into DMF solution after one week. Yield: 0.13 g (0.056 mmol, 21 %). ^{1}H NMR (400 MHz, [D$_6$]DMSO): δ = 0.86 (t, 6H; -CH$_3$), 0.94 (t, 36H; TBA), 1.24 (s, 56H; -CH$_2$-), 1.32 (m, 24H; TBA), 1.57 (m, 24H; TBA), 3.17 ppm (m, 24H; TBA); IR (KBr, cm^{-1}): $\tilde{\nu}$ = 3432 (w), 2927 (s), 2873 (m), 1670 (m), 1549 (m), 1479 (m), 1383 (w), 1032 (m), 941 (s), 922 (s), 667 cm^{-1} (vs); ESI-MS (negative mode, MeCN): 937 g mol^{-1} ([M-2DMF-7H$_2$O-2TAB]$^{2-}$); elemental analysis calcd (%) for C$_{88}$H$_{184}$MnMo$_6$N$_5$O$_{26}$·7H$_2$O·2DMF (2631.3 g mol^{-1}): C 42.91, H 8.12, N 3.73; found: C 42.62, H 7.73, N 3.89.

Synthesis of [(nC$_4$H$_9$)$_4$N]$_3$[MnMo$_6$O$_{18}${(OCH$_2$)$_3$CNH-CO-(CH$_2$)$_{16}$CH$_3$}$_2$]·2DMF (compound 4): Compound **1** (0.50 g; 0.27 mmol) and Et$_3$N (150 μL; 0.109 g; 1.08 mmol) were dissolved in 30 mL of acetonitrile. Stearoyl chloride (0.16 g; 0.53 mmol) was added and the solution was set to reflux for 18 h. A white precipitate was filtered off and the solvent was evaporated. The solid orange residue was dissolved in a minimum amount of dry DMF and further white precipitate was filtered off. After three days of slow evaporation at room temperature, small orange crystals could be obtained. Yield: 0.17 g (0.067 mmol, 25 %). ^{1}H NMR (400 MHz, [D$_6$]DMSO, 25 °C): δ = 0.86 (t, 6H; -CH$_3$), 0.94 (t, 36H; TBA), 1.24 (s, 64H; -CH$_2$-), 1.34 (m, 24H; TBA), 1.57 (m, 24H; TBA), 3.171 ppm (m, 24H; TBA); IR (KBr, cm^{-1}): $\tilde{\nu}$ = 3462 (m), 2925 (s), 2854 (m), 1670 (m), 1550 (w), 1483 (m), 1382 (w), 1027 (m), 941 (s), 921 (s), 666 ppm (vs); ESI-MS (negative mode, MeCN): 965 g mol^{-1}, ([M-2DMF-3H$_2$O-2TAB]$^{2-}$); elemental analysis calcd (%) for C$_{92}$H$_{192}$MnMo$_6$N$_5$O$_{26}$·2DMF·3H$_2$O (2615.3 g mol^{-1}): C 45.01, H 8.17, N 3.75; found: C 45.20, H 8.07, N 3.81.

Synthesis of [DMDOA]$_3$[MnMo$_6$O$_{18}${(OCH$_2$)$_3$CNH-CO-(CH$_2$)$_{14}$CH$_3$}$_2$]·2DMF·4H$_2$O (compound 5): The crystalline powder of compound **2** (150 mg, 0.057 mmol) was dissolved in 15 mL of MeCN and the solution was kept stirring for 30 min, then it was added dropwise to the clear solu-

tion of excess amount (1.80 g, 2.85 mmol) of dimethyldiocta-decylammonium bromide (DMDOABr) in a mixture of CHCl₃ and MeCN (1:3, 50 mL). Yellow-orange precipitates were formed immediately and filtered, dried under vacuum overnight. Yield: 0.17 g (0.048 mmol, 85%). ESI-MS (negative mode, MeCN) 2801 g mol⁻¹ ([M-2DMF-4H₂O-2TBA+H⁺]⁻); elemental analysis calcd (%) for C₁₅₄H₃₁₆MnMo₆N₅O₂₆·2DMF·4H₂O (3503 g mol⁻¹): C 54.86, H 9.73, N 2.80; found C 54.55, H 9.30. N 2.74.

Synthesis of [DMDOA]₃[MnMo₆O₁₈{(OCH₂)₃CNH-CO-(CH₂)₁₆CH₃}₂] ·2DMF·4H₂O (compound 6): is similar to that of compound **5**, only compound **3** is used here as the starting material instead of compound **2**. Yield: 70%. ESI-MS (negative mode, MeCN) 2829 g mol⁻¹ ([M-2DMF-4H₂O-2TBA+H⁺]⁻); elemental analysis calcd (%) for C₁₅₆H₃₂₀MnMo₆N₅O₂₆·2DMF·4H₂O (3531 g mol⁻¹): C 55.10, H 9.76, N 2.78; found C 54.58, H 9.66. N 2.68.

[1] D.-L. Long, E. Burkholder, L. Cronin, *Chem. Soc. Rev.* **2007**, *36*, 105.

[2] B. Hasenknopf, *Front. Biosci.* **2005**, *10*, 275.

[3] N. Mizuno, K. Yamaguchi, K. Kamata, *Coord. Chem. Rev.* **2005**, *249*, 1944.

[4] Y.-F. Song, D.-L. Long, L. Cronin, *Angew. Chem.* **2007**, *119*, 3974; *Angew. Chem.* **2007**, *119*, 3974; *Angew. Chem. Int. Ed.* **2007**, *46*, 3900.

[5] Z. H. Peng, *Angew. Chem.* **2004**, *116*, 948; *Angew. Chem.* **2004**, *116*, 948; *Angew. Chem. Int. Ed.* **2004**, *43*, 930.

[6] S. Bareyt, S. Piligkos, B. Hasenknopf, P. Gouzerh, E. Lacote, S. Thorimbert, M. Malacria, *J. Am. Chem. Soc.* **2005**, *127*, 6788.

[7] C. Boglio, G. Lenoble, C. Duhayon, B. Hasenknopf, R. Thouvenot, C. Zhang, R. C. Howell, B. P. Burton-Pye, L. C. Francesconi, E. Lacote, S. Thorimbert, M. Malacria, C. Afonso, J. C. Tabet, *Inorg. Chem.* **2006**, *45*, 1389.

[8] C. R. Mayer, R. Thouvenot, *J. Chem. Soc. Dalton Trans.* **1998**, 7.

[9] A. Mazeaud, N. Ammari, F. Robert, R. Thouvenot, *Angew. Chem*, **1996**, *108*, 2089; *Angew. Chem.* **1996**, *108*, 2089; *Angew. Chem. Int. Ed. Engl.* **1996**, *35*, 1961; D. Agustin, J. Dallery, C. Coelho, A. Proust, R. Thouvenot, *Organomet. Chem* **2007**, *692*, 746.

[10] C. Sanchez, G. J. D. A. Soler-Illia, F. Ribot, T. Lalot, C. R. Mayer, V. Cabuil, *Chem. Mater.* **2001**, *13*, 3061.

[11] H. L. Li, H. Sun, W. Qi, M. Xu, L. X. Wu, *Angew. Chem*, **2007**, *119*, 1322; *Angew. Chem.* **2007**, *119*, 1322; *Angew. Chem. Int. Ed.* **2007**, *46*, 1300; D. Fan, X. Jia, P. Tang, J. Hao, T. Liu. *Angew. Chem.* **2007**, *119, 3406; Angew. Chem. Int. Ed.* **2007**, 46, 3342; *Angew. Chem. Int. Ed.* **2007**, *46*, 3342.

[12] H. L. Li, W. Qi, W. Li, H. Sun, W. F. Bu, L. X. Wu, *Adv. Mater.* **2005**, *17*, 2688.

[13] W. Li, W. F. Bu, H. L. Li, L. X. Wu, M. Li, *Chem. Commun.* **2005**, 3785.

[14] L. Wang, J. Li, E. B. Wang, L. Xu, J. Peng, Z. Li, *Mater. Lett.* **2004**, *58*, 2027.

[15] L. Cheng, L. Niu, J. Gong, S. J. Dong, *Chem. Mater.* **1999**, *11*, 1465.

[16] M. Ruben, J. M. Lehn, P. Muller, *Chem. Soc. Rev.* **2006**, *35*, 1056.

[17] C. Cannizzo, C. R. Mayer, F. Secheresse, C. Larpent, *Adv. Mater.* **2005**, *17*, 2888.

[18] J. C. Love, L. A. Estroff, J. K. Kriebel, R. G. Nuzzo, G. M. Whitesides, *Chem. Rev.* **2005**, *105*, 1103.

[19] G. M. Whitesides, M. Boncheva, *Proc. Natl. Acad. Sci. USA* **2002**, *99*, 4769.

[20] F. J. M. Hoeben, I. O. Shklyarevskiy, M. J. Pouderoijen, H. Engelkamp, L. P. H. J. Schenning, P. C. M. Christianen, J. C. Maan, E. W. Meijer, *Angew. Chem.*, **2006**, *118*, 1254; *Angew. Chem.* **2006**, *118*, 1254; *Angew. Chem. Int. Ed.* **2006**, *45*, 1232.

[21] I. O. Shklyarevskiy, P. Jonkheijm, P. C. M. Christianen, A. P. H. J. Schenning, E. W. Meijer, O. Henze, A. F. M. Kilbinger, W. J. Feast, A. Del Guerzo, J. P. Desvergne, J. C. Maan, *J. Am. Chem. Soc.* **2005**, *127*, 1112.

[22] S. Q. Zhou, C. Burger, B. Chu, M. Sawamura, N. Nagahama, M. Toganoh, U. E. Hackler, H. Isobe, E. Nakamura, *Science* **2001**, *291*, 1944.

[23] P. Garcia, J. Marques, E. Pereira, P. Gameiro, R. Salema, B. de Castro, *Chem. Commun.* **2001**, 1298.

[24] P. R. Marcoux, B. Hasenknopf, J. Vaissermann, P. Gouzerh, *Eur. J. Inorg. Chem.* **2003**, 2406.

[25] S. Favette, B. Hasenknopf, J. Vaissermann, P. Gouzerh, C. Roux, *Chem. Commun.* **2003**, 2664.

[26] Crystal data and structure refinements for compound **2**: C₇₄H₁₆₀MnMo₆N₇O₂₉ M=2242.67 g mol⁻¹; an orange, crystal (0.16× 0.16×0.16 mm³) was measured on a Bruker Apex II CCD diffractometer using Mo$_{Kα}$ radiation (λ=0.71073 Å) at 100(2) K. Orthorhombic, space group $Pna2_1$, a=18.5540(8) Å, b=20.2839(8) Å, c= 26.0613(11) Å, V=9808.1(7) Å³, Z=4, 18510 unique, 17243 observed (I>2σ(I)). $R1$=0.0281, $wR2$ (all data)=0.0744. Compound **3**: C₉₄H₂₁₂MnMo₆N₇O₃₅ M=2631 g mol⁻¹; an orange, crystal (0.10× 0.03×0.03 mm³). Monoclinic, space group $C2/c$, a=49.590(10) Å, b=28.512(6) Å, c=25.585(5) Å, β=99.78(3), V=35649(12) Å³, Z= 12, 32869 unique, 24464 observed (I>2σ(I)). $R1$=0.198, $wR2$ (all data)=0.503. CCDC 649359 (**2**) and 649360 (**3**) contain the supplementary crystallographic data for this paper. These data can be obtained free of charge from The Cambridge Crystallographic Data Centre via www.ccdc.cam.ac.uk/data_request/cif.

[27] P. C. Schulz, J. L. Rodriguez, F. A. Soltero-Martinez, J. E. Puig, Z. E. Proverbio, *J. Therm. Anal. Calorim.* **1998**, *51*, 49.

[28] J. H. Fendler, *Acc. Chem. Res.* **1980**, *13*, 7.

[29] M. J. Blandamer, B. Briggs, P. M. Cullis, S. D. Kirby, J. B. F. N. Engberts, *J. Chem. Soc. Faraday. Trans.* **1997**, *93*, 453.